

Online support information for:

Decoupling the Role of Lignin, Cellulose/Hemi-cellulose, and Ash on ZnCl₂-Activated Carbon Pore Structure

Chengjun Wu, Graham W. Tindall, Carter L. Fitzgerald, Mark C. Thies[^], Mark E. Roberts^{^*}

Department of Chemical and Biomolecular Engineering, 127 Earle Hall, Clemson University, Clemson, South Carolina, 29634-0909, United States of America

*Corresponding author. Tel: 864 656-6307. E-mail: mrober9@clemson.edu

Lignin-rich waste streams from a lignocellulosic biorefinery process (Hybrid Poplar feed) were separated into samples with varying sugars and ash content using a two-step Aqueous Lignin Purification using Hot Agents process (details provided in Section 2.1).

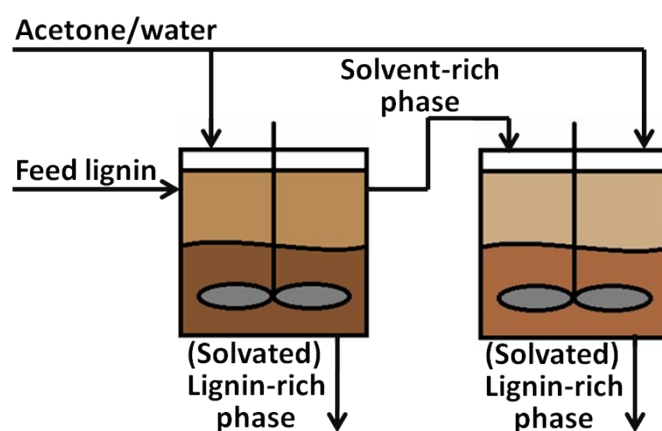


Figure S1. Two-stage ALPHA process for separating lignin-rich waste streams into biomass samples with varying sugars and ash content.

Table S1 shows the results of the inductively coupled plasma atomic emission spectroscopy (ICP-AES) analysis for the two feed samples - the bulk lignin feed (BLF) and lignin cake feed (LCF). The elemental content in each sample is based on weight percentage. The lignin rich stream remaining after enzymatic digestion, LCF, contains almost 6x the total metal from the lignin-rich stream remaining after the alkali pretreatment, BLF. Sodium is the primary metal in the BLF stream, accounting for nearly 90% of the total metal content by weight. Calcium is the most abundant metal in the LCF stream, representing almost 80% of the total metal content by weight. The sulfur content in both feed streams is relatively low, each less than 0.1 wt%, of the respective sample. Lignin rich streams produced from the Kraft process typically have higher sulfur, 1-3 wt%, because of the sulfur-containing chemical involved; here, the alkali pretreatment was carried out with NaOH.

Table S1. Inductively Coupled Plasma Atomic Emission Spectroscopy Result of Bulk Lignin Feed and Lignin Cake Feed.

Sample	P	K	Ca	Mg	Zn	Cu	Mn	Fe	S	Na	Total Metals [ppm]
BL Feed	34.6	69.4	34.1	4.7	3.3	4.9	0.2	20.6	974.2	927.4	1064.6
LC Feed	79.6	236.6	4741.9	643.2	16.0	6.6	2.8	58.5	441.4	481.0	6186.6

Table S2 presents the sugar content in each biomass sample, expressed in terms of monomer composition, which is determined via high-performance liquid chromatography (HPLC). Due to the digestion process involved in polysaccharide analysis, the results are shown as monosaccharide content. The BLF and the LCF, which are derived from different lignin extraction stages, primarily contain different types of sugars. In the BLF stream, the main sugar is xylan, a monomer of hemicellulose. The LCF primarily contains monomers of cellulose, as evidenced by the glucose detected in the polysaccharide results. The sugars present in the fractionated samples mirror those of their respective feeds; however, their sugar contents differ due to the fractionation through the ALPHA process.

Table S2. Xylose contents (wt %), Arabinose contents(wt %), glucose contents(wt %) and total sugar compositions(wt %) of biomass samples.

Sample	Xylose Content (Wt %)	Arabinose Content (Wt %)	Glucose Content (Wt %)	Total Sugar Content (Wt %)
BLF	1.7	<0.1	0.2	2.0
α LR-a	9.2	<0.1	1.0	10.2
α LR-b	13.6	0.4	2.0	15.9
α LR-c	24.7	0.6	3.5	28.8
α LP	<0.1	<0.1	<0.1	<0.1
α 2LR	<0.1	<0.1	<0.1	<0.1
LCF	3.6	0.4	22.9	26.9
LCR	0.2	<0.1	55.4	55.6
LCL	0.2	<0.1	1.5	1.7

Figure S2 shows the carbon fraction in the biomass samples and activated carbon (AC), as well as the carbon fractional conversion. The carbon fraction, determined by the elemental analysis of combustion products, is based on weight fraction. The carbon fractional conversion is calculated by dividing the mass of carbon in AC by the mass of carbon in the starting biomass sample. According to the figure, the carbon fraction in AC is fairly consistent, ranging between 87% and 89%. However, the carbon fraction in the biomass sample varies due to differences in sugar content.

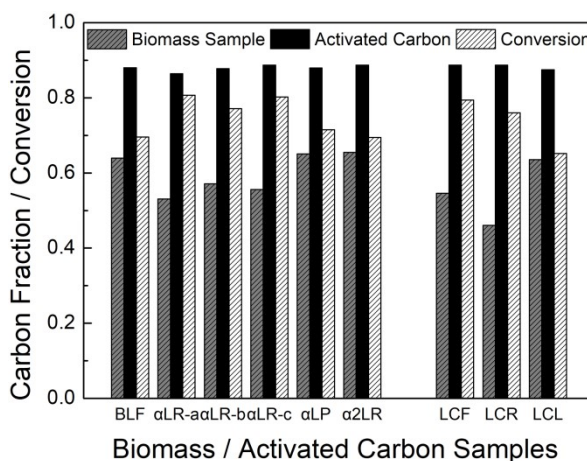


Figure S2. Carbon fractions (weight fraction) in biomass samples (dark grey) and ACs (black). Fractional

conversions of carbon (light grey) from biomass samples into the AC products.

Figure S3 displays the adsorption-desorption isotherms of samples with varying sugar composition (panel a) and varying ash content (panel b). In panel a, the N_2 adsorption amount of AC correlates with the sugar composition in sample, which increases as the sugar composition increases. This indicates that pores more easily form in samples with increasing sugar content. The type I/II isotherms suggest that these activated carbons contain a combination of slit-type mesopores and micropores. The type H4 hysteresis loops that appear in samples with lower sugar composition suggest that the pores also exhibit a micro-mesoporous structure, and that the pores may be pinched at the entrances. In panel b, it is noticeable that the size of the hysteresis loop increases with the increasing ash content for all samples that have a relatively low amount of sugar. This supports the mechanism of pore growth because the ash blocks the $ZnCl_2$ from penetrating into the particles. When the sugar composition exceeds 20%, the effect of ash content becomes insignificant as the hysteresis loop disappears. All of the individual isotherms are shown separately in Figure S4.

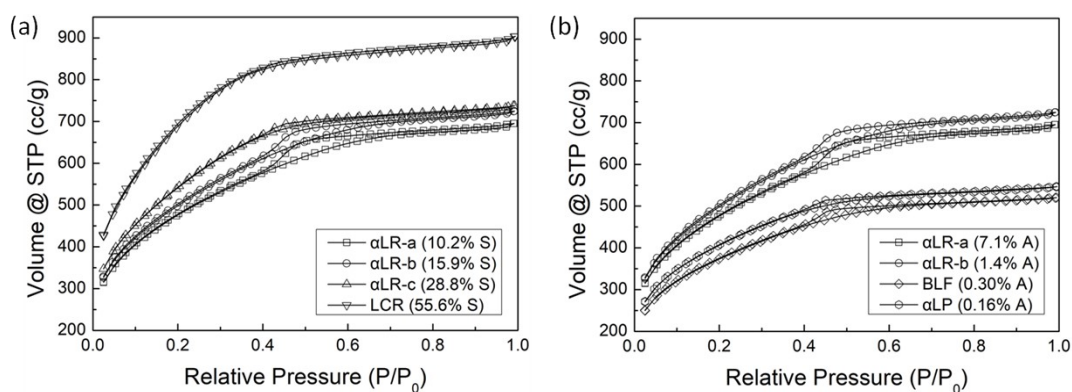


Figure S3. N_2 adsorption-desorption isotherms of ACs from biomass samples with (a) varying sugar composition and (b) varying ash content.

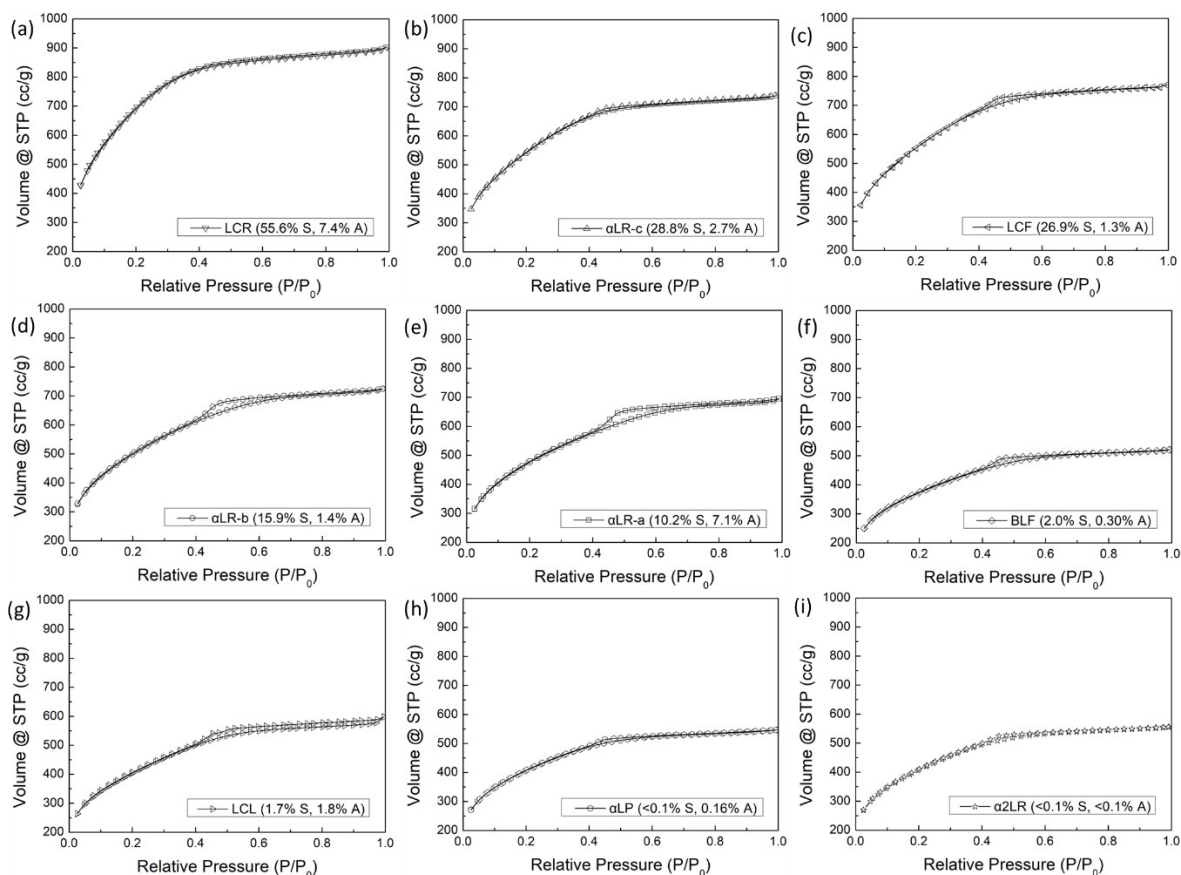


Figure S4. N₂ adsorption-desorption isotherms of ACs from all biomass samples.

Figure S5 shows the pore size distribution of two samples that have similar sugar compositions but different ash content. Despite the fact that the ash content of the α LR-c sample is more than twice that of the LCF sample (2.7% vs 1.3%), the α LR-c sample, with a marginally higher sugar content (28.8% vs 26.9%), exhibits fewer mesopores (with a pore width of 3.6 nm). This means that the sugar composition has a more significant impact on pore properties than the ash content. If ash was the primary driver of pore formation, we would expect the observed trend to be reversed.

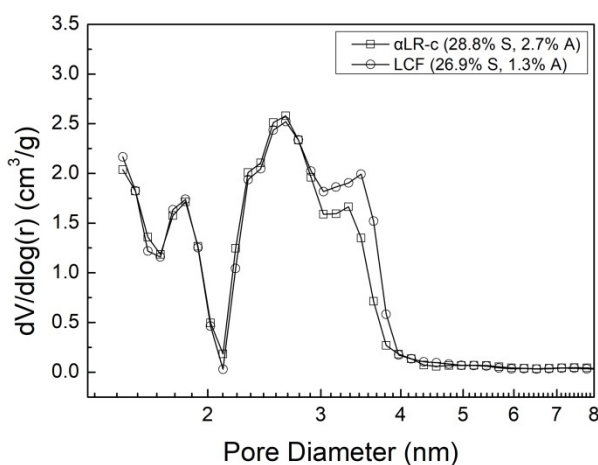


Figure S5. Pore size distribution in AC from biomass samples of α LR-c (line + hollow square) and LCF (line + hollow circle)